Plasma Wave Observations near the Plasmapause with the S³-A Satellite

ROGER R. ANDERSON AND DONALD A. GURNETT

Department of Physics and Astronomy, The University of Iowa
Iowa City, Iowa 52240

Summary. In this paper we describe the electric field noise phenomena observed by the S³-A spacecraft near the plasmapause during the magnetic storm of December 16–17, 1971. The most striking and unusual feature of these storm time electric field observations is the occurrence of a region of intense low-frequency (20 to 500 Hz) electrostatic noise bursts just outside the plasmapause boundary. These noise bursts occurred concurrent with the rapid decrease in low-energy ($20 \lesssim E \lesssim 50$ kev) ring current protons mirroring near the equator during this storm and may be responsible for the loss of these particles. The characteristics of other phenomena, such as whistlers, ELF hiss, and banded chorus, observed near the plasmapause during this period are also discussed.

The charged-particle and magnetic field experiments on the Small Scientific Satellite, S³-A, have provided a comprehensive survey of the plasma and magnetic field variations during the December 16–17, 1971, magnetic storm, the results of which are presented in a companion set of papers. The purpose of this paper is to describe the electric field noise phenomena observed at selected periods during this storm by the University of Iowa electric field experiment on S³-A.

Of particular interest during this storm is the observation of intense low-frequency (20 to 500 Hz) electrostatic noise as the satellite crosses into the plasmasphere at about $L = 3.4$ on orbit 99. This noise occurs concurrent with the steep intensity gradients observed in the low-energy ring current protons. *Williams et al.* [1973] observe the steepest decrease for the $35.1 \leq E \leq 50.4$ kev protons at $L = 4.0$ and for the $22.3 \leq E \leq 30.2$ kev protons at $L = 3.4$. The onset of the decrease in proton intensities has been attributed by *Williams et al.* [1973] to pitch angle scattering by ion cyclotron turbulence, as suggested by *Cornwall et al.* [1970]. *Cornwall et al.* [1971] predicted wave frequencies for the ion cyclotron turbulence near the magnetic equator to be from 0.33 to 0.75 of the proton cyclotron frequency. The proton cyclotron frequency at the inbound plasmapause crossing of orbit 99 was about 13 Hz, thus indicating that the ion cyclotron turbulence should be at a frequency of about 4 to 10 Hz. Electric field signals in the 1- to 30-Hz ranges were observed on this orbit near the plasmapause by *Maynard and Cauffman* [1973]. However, no magnetic field signals above the search coil magnetometer's sensitivity ($\sim$0.1 to 0.2 γ in the 4- to 10-Hz range) were simultaneously observed [*Parady and Cahill*, 1973]. Because electric field signals from 20 to 500 Hz were observed near the plasmapause to be more intense than the 1- to 30-Hz signals and because no electromagnetic ion cyclotron turbulence above the noise level of the search coil magnetometer was detected, our primary objective in this paper is to investigate the electric field noise phenomena in this region of steep proton intensity gradients in order to determine if an electrostatic instability, such as was recently suggested by *Coroniti et al.* [1972], could be responsible for the observed proton intensity decreases.

INSTRUMENTATION

The satellite S³-A was launched from the San Marco Equatorial Range, Kenya, Africa, on November 15, 1971, into an eccentric equatorial orbit. The perigee altitude was 222 km, the apogee altitude was 27,031 km (5.24 R_E geocentric), the inclination was 3.57°, and the orbital period was 7 hours 49 min. S³-A was spin-stabilized with the spin axis near the ecliptic plane. The electric dipole antenna on S³-A con-

sists of two graphite-coated spheres, 14 cm in diameter, mounted on booms such that the center-to-center distance between the spheres is 5.08 meters. Each sphere is connected to a high input impedance ($C_{in} \simeq 10$ pf, $R_{in} \simeq 50$ megohms) unity gain preamplifier mounted on the boom about halfway between the center of the sphere and the center of the spacecraft. The axis of the electric dipole antenna is perpendicular to the spacecraft spin axis.

The electronics instrumentation for the University of Iowa electric field experiment consists of two principal elements: (1) a step frequency spectrum analyzer, and (2) a wideband receiver. The step frequency spectrum analyzer has 15 narrowband frequency channels with center frequencies logarithmically spaced from 35 Hz to 100 kHz and one wideband frequency channel with a bandpass of about 100 Hz to 10 kHz. The four highest frequency narrowband filters of the step frequency analyzer have bandwidths of $\pm 7.5\%$ of their center frequencies, and the remaining narrowband filters have bandwidths of $\pm 15.0\%$ of their center frequencies. A differential amplifier is used to provide a signal proportional to the potential difference between the antenna elements. The differential amplifier output signal drives all of the filters simultaneously. The filter outputs are then sequentially switched into an 80-db logarithmic detector to provide frequency spectrum measurements. The logarithmic detector output is a dc voltage proportional to the logarithm of the average input amplitude. The reprogrammable onboard data system controls the switching of the spectrum analyzer filters and the sampling of the logarithmic detector output.

The wideband receiver is an 80-db automatic gain control (AGC) receiver with a bandwidth of about 100 Hz to 10 kHz. The output of the wideband receiver modulates the special purpose telemetry transmitter. The wideband data are recorded on the ground and then are processed by a spectrum analyzer to produce high-resolution frequency-time spectrograms. The wideband system is normally operated one orbit out of three but can be operated continuously for special periods.

OBSERVATIONS

Inbound orbit 99, during which the low-frequency electrostatic noise was observed near the plasmapause boundary, occurred on December 17, 1971, during the initial phase of the magnetic storm. The apogee of this orbit was located at about 21.0 hours local time. *Maynard and Cauffman* [1973] have identified the inbound plasmapause crossing on this orbit from the dc potential difference between the spheres, which changes abruptly at the plasmapause boundary. From their data, which are reproduced in panel (*c*) of Figure 1, they determined that the inbound plasmapause crossing on orbit 99 occurred at about 0615 UT and $L = 3.4$. Several features of the wideband data that support this determination of the plasmapause location are discussed later in this paper.

Panel (*d*) of Figure 1 shows the electric field amplitudes for the eight lowest frequency channels (35 Hz to 1.78 kHz) near the inbound plasmapause crossing of orbit 99. The electric field amplitudes plotted are the peak rms electric field amplitudes obtained over successive 67-sec intervals. Peak values are shown in order to eliminate the modulation due to the spacecraft spin and to provide a quantitative indication of the amplitude of impulsive noise bursts that otherwise would not be as evident. The electric field amplitudes have been computed by assuming that the effective length of the electric dipole antenna is equal to the separation distance between the spheres (5.08 meters). Panels (*a*) and (*b*) of Figure 1 show frequency-time spectrograms of the wideband magnetic and electric fields, respectively.

Figure 1 shows that several features of the electric field noise change markedly near the plasmapause boundary at 0615 UT. In the 35- and 62-Hz frequency channels, it is evident that the electric field amplitudes decrease by more than an order of magnitude as the spacecraft crosses into the plasmasphere. Outside the plasmasphere at about 0600 UT, the electric field amplitudes in the 35- and 62-Hz channels are about 500 and 100 μv (meter)$^{-1}$, respectively, and inside the plasmapause at about 0616 UT, the corresponding electric field amplitudes have decreased to about 30 and 7.0 μv (meter)$^{-1}$, respectively. Since similar changes have been observed both before and during a magnetic storm, this change in the electric field amplitudes in the 35- and 62-Hz channels, and to a smaller extent in the 120-Hz channel, is apparently a characteristic feature of the plasmapause bound-

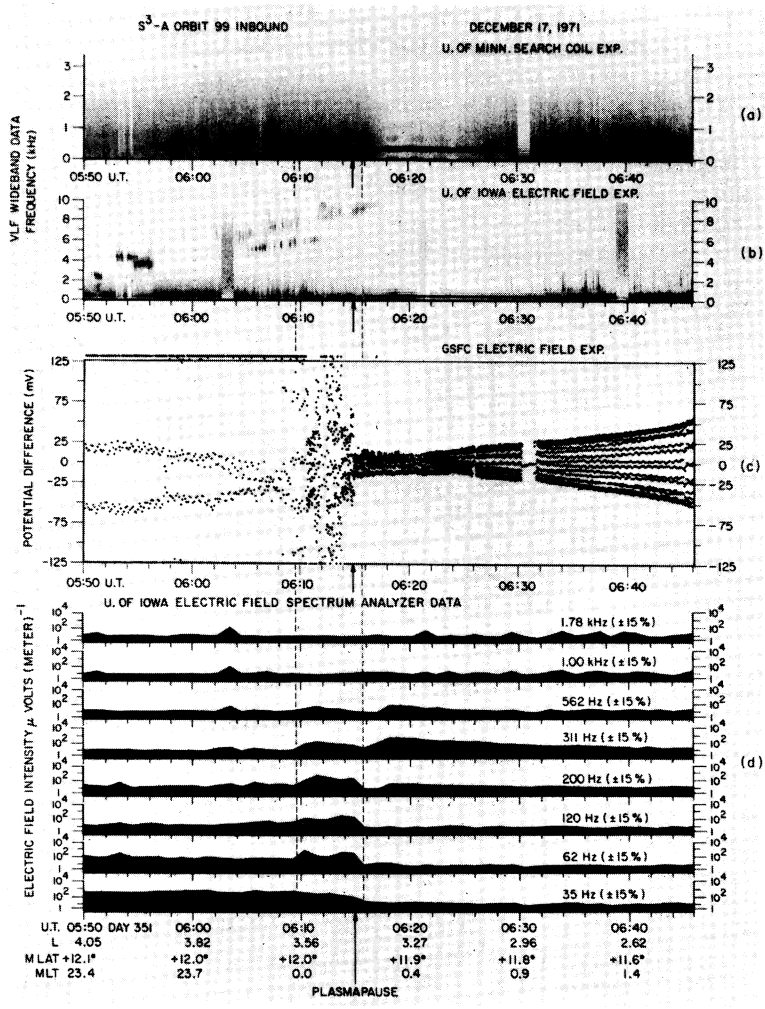

Fig. 1. Four sets of field observations for inbound orbit 99 in the vicinity of the plasmapause. All four panels contain data for the same 56-min time period from 0550 to 0646 UT on December 17, 1971. Panel (*a*) is a 0-Hz to 3-kHz frequency-time spectrogram of the magnetic field wideband data. Panel (*b*) is a 0-Hz to 10-kHz frequency-time spectrogram of the electric field wideband data. Panel (*c*) is a plot of the dc potential difference between the spheres. Panel (*d*) contains plots of the peak amplitudes measured for the eight lowest frequency channels of the University of Iowa's electric field experiment onboard spectrum analyzer. *Williams et al.* [1973] observe the steepest decrease for the $35.1 \leq E \leq 50.4$ kev protons at about 0550 UT and for the $22.3 \leq E \leq 30.2$ kev protons near the plasmapause at about 0615 UT. The region indicated by the dashed lines is where the enhancement in the low-frequency electric field noise is most intense.

ary and does not appear to be related to the occurrence of a magnetic storm except for the location of the plasmapause.

An even more pronounced enhancement in the low-frequency electric field noise, which is confined to the immediate vicinity of the plasmapause, is evident in Figure 1 between the vertical dashed lines at 06h09m30s and 06h15m40s UT. The maximum electric field amplitudes in the 62-, 120-, 200-, and 311-Hz frequency channels during this period are nearly an order of magnitude greater than the corresponding amplitudes farther outside the plasmapause. A similar but smaller enhancement is also evident in the 562-Hz frequency channel. By comparing these data with the low-energy ($20 \lesssim E \lesssim 50$ kev)

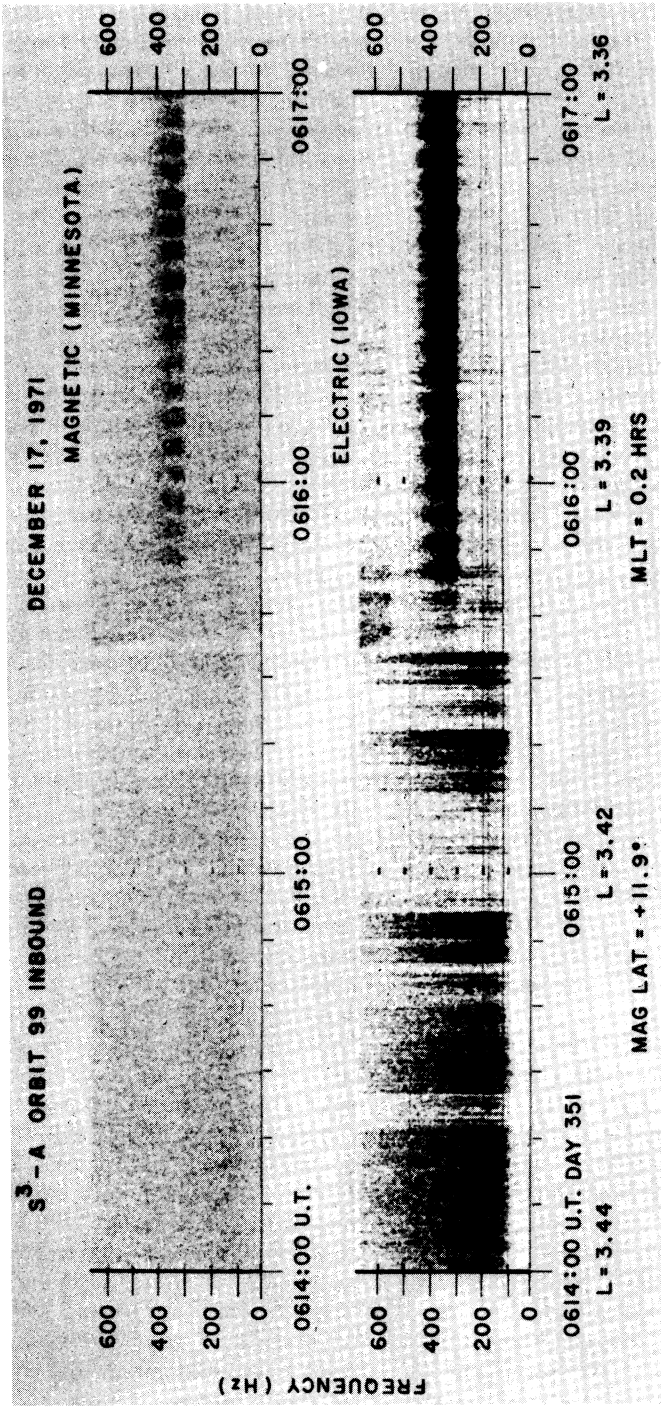

Fig. 2. The upper panel is a 0- to 650-Hz frequency-time spectrogram of the magnetic field wideband data. The lower panel is a 0- to 650-Hz frequency-time spectrogram of the electric field wideband data. Both panels are for the same 3-min period near the plasmapause. Note that the intense vertical bursts from 06h14m00s to 06h15m40s UT occur only in the electric field data. The ELF hiss band from about 300 to 420 Hz, which begins at 06h15m37s UT, is present in both the electric and the magnetic field data. Analysis of the spin modulation of the ELF hiss band determined that the hiss is propagating nearly perpendicular to the geomagnetic field. The ELF hiss band has the same well-defined frequency limits for more than 30 min as the satellite moves inward more than 1 R_E.

proton intensities reported by *Williams et al.* [1973] for this orbit, it is seen that this low-frequency electric field noise enhancement corresponds closely with the region of rapidly decreasing proton intensities at the inner edge of the ring current.

Expanded 0- to 650-Hz frequency-time spectrograms of the electric and magnetic fields near the plasmapause boundary are shown in Figure 2 for the period from 0614 to 0617 UT. The horizontal lines are ground-based interference acquired during the recording and processing of the data. The large number of nearly vertical bursts of ~0.25-sec or less duration extending until approximately 06h15m40s UT in Figure 2 correspond to the enhanced low-frequency electric field noise intensities between the vertical dashed lines in Figure 1. These bursts are bunched in groups that last from a few seconds to several tens of seconds. The bursts occasionally extend to nearly 600 Hz but are usually most intense below 300 Hz. The lower frequency cutoff at about 100 Hz is due to the lower frequency limit of the wideband receiver. These low-frequency noise bursts are not observed in the magnetic spectrogram (top panel of Figure 2), nor are they observed in the narrowband data from the search coil magnetometer [*Parady and Cahill*, 1973]. Although the low-frequency noise bursts are most intense and rise to higher frequencies in the period from 06h09m30s to 06h15m40s UT, the same type of noise bursts is also observed before 06h09m30s UT. These low-frequency noise bursts have also been observed on other orbits during this storm and have been either of much lower intensity or entirely absent during magnetically quiet periods.

Several features of the wideband data are similar to features found near the plasmapause by other satellites. In Figures 1 and 3 at 06h15m33s UT, slightly inside the plasmapause (as determined by the GSFC electric field experiment), the first long hop whistler of this inbound pass is observed, similar to the results of *Carpenter et al.* [1969]. Further inside the plasmapause, at 06h15m37s UT, an ELF hiss band is observed corresponding to the 'plasmaspheric hiss' discussed by *Russell and Holzer* [1970] and *Carpenter et al.* [1969]. As seen from Figure 2, this ELF hiss emission is confined to a narrow frequency band from about 300 to 420 Hz. These frequency limits do not vary for the entire time of observation, which suggests that the noise is being generated at a specific point and then is propagating to other regions. As seen in panel (*d*) of Figure 1, the electric field strength in the 311-Hz frequency channel is 50 μv (meter)$^{-1}$ at 0616 UT, increases to 580 μv (meter)$^{-1}$ at 0618 UT, and slowly decreases to 26 μv (meter)$^{-1}$ at 0646 UT. As can be seen in Figure 2, the amplitude of the ELF hiss has a pronounced spin modulation. The nulls in the magnetic field intensity occur when the search coil axis is perpendicular to the geomagnetic field. The nulls in the electric field intensity occur when the electric dipole axis is parallel to the geomagnetic field. This field geometry implies that the ELF hiss is propagating nearly perpendicular to the geomagnetic field. We are currently attempting to determine the Poynting flux direction of this noise from the relative phase of the electric and magnetic antenna signals.

At higher frequencies, above about 1 kHz, the predominant phenomena observed outside the plasmapause is banded chorus of the type described by *Burtis and Helliwell* [1969]. Several sporadic bursts of banded chorus are evident in panel (*b*) of Figure 1 before 0556 UT at a frequency of about 4 kHz. Later, two well-defined bands of banded chorus are evident. The lower frequency band begins at about 0605 UT and ends at about 0615 UT. The higher frequency band begins at about 0602 UT and moves out of the passband of the wideband receiver at 0618 UT. The frequency of these bands increases systematically with decreasing altitude. In the onboard spectrum analyzer data, the higher band is observed in the 10.0-kHz (±15%) frequency channel until 0627 UT and in the 16.5-kHz (±7.5%) frequency channel at 0632 UT. The center frequency of the lower frequency band is about 0.27 of the measured local electron cyclotron frequency from 0605 to 0615 UT. The center frequency of the higher frequency band is about 0.36 of the measured local electron cyclotron frequency from 0602 to 0618 UT. The frequency-time character of the discrete emissions that form these bands is illustrated in the expanded time-scale spectrograms of Figures 3 and 4. The lower band consists of nearly vertical emissions of 0.25 sec or less in duration with a bandwidth of about 1 kHz. Before about 0614 UT, the higher band consists of intense vertical bursts similar to those in the lower band; however, these bursts are

Fig. 3. A 0-Hz to 10-kHz frequency-time spectrogram of the electric field wideband data near the plasmapause. The first whistler on inbound orbit 99 is observed at 06h15m33s UT just inside the plasmapause. The ELF hiss band described in Figure 2 begins shortly after the whistler observation. The low-frequency electric field noise bursts, which are most intense from 06h15m10s to 06h15m35s UT, are shown expanded in frequency in Figure 2. Banded chorus is observed above 8.5 kHz and consists of a band of diffuse noise bursts in contrast to that observed in Figure 4 only 4 min earlier.

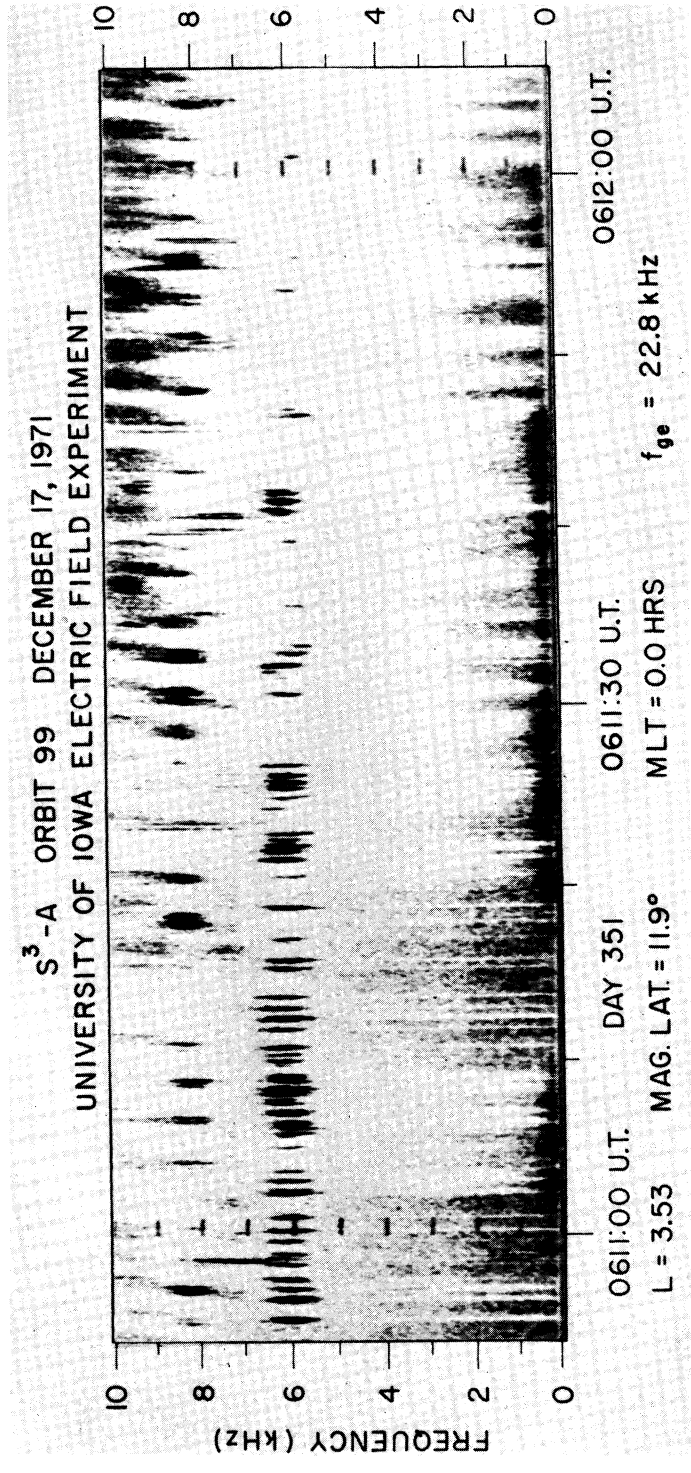

Fig. 4. A 0-Hz to 10-kHz frequency-time spectrogram of the electric field wideband data just outside the plasmapause. Intense low-frequency noise bursts are evident up to 500 Hz for tens of seconds. The discrete emissions near 6.0 and 8.0 kHz are banded chorus. The upper band has diffuse noise following each emission. In Figure 3 just 4 min later only diffuse noise above 8.5 kHz is present.

followed by a rising diffuse noise of about 1-sec duration, as can be seen in Figure 4. Beginning at about 0615 UT, the intense vertical bursts disappear and the higher band consists only of diffuse noise in the same frequency range where the vertical bursts previously occurred. Banded chorus has been observed on most passes that go outside of the plasmasphere.

To summarize the electric field noise intensities observed during orbit 99, the electric field spectral densities measured by S³-A over the frequency range from 1 Hz to 100 kHz are shown in Figure 5 for three representative locations: (1) outside of the plasmasphere at $L = 3.87$, (2) near the plasmapause at $L = 3.44$, and (3) inside the plasmasphere at $L = 3.30$. The data from 1 to 30 Hz were provided by Nelson Maynard from the GSFC electric field experiment on S³-A. Above about 1 kHz, the electric field spectral densities do not vary greatly across the plasmapause except for the occurrence of banded chorus near and outside the plasmapause. With the exception of the ELF hiss band at about 300 Hz, the electric field spectral densities at frequencies below about 1 kHz are generally much larger outside the plasmapause than inside. At frequencies below about 100 Hz, this large increase in the electric field intensity outside of the plasmapause may be partly attributed to harmonics of the spacecraft spin rate that are generated by asymmetrical spacecraft sheath effects outside of the plasmapause. Near the plasmapause (at $L = 3.44$ in Figure 5), the main contribution to the broadband electric field strength comes from the broad peak in the electric field spectral density that extends from

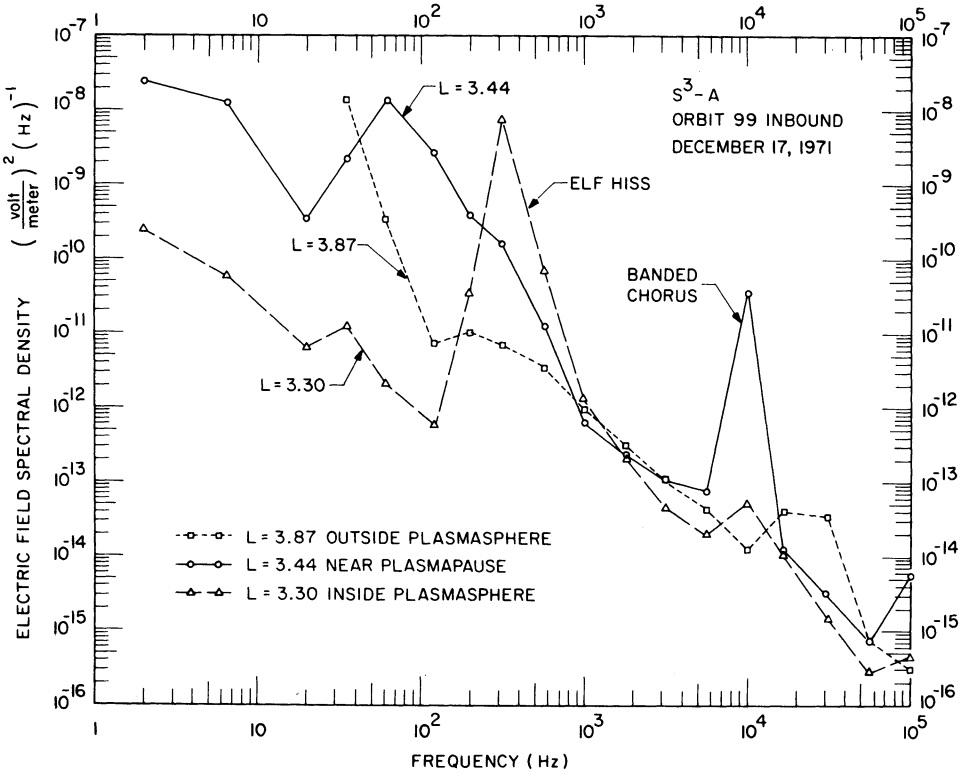

Fig. 5. The electric field spectral density from 1 Hz to 100 kHz for measurements made outside the plasmasphere at $L = 3.87$, near the plasmapause at $L = 3.44$, and inside the plasmasphere at $L = 3.30$. The broad peak from 20 to 500 Hz for $L = 3.44$ is a result of the low-frequency electric field noise bursts shown in Figure 2. The maximum integrated rms electric field strength for these noise bursts is about 1 mv (meter)$^{-1}$. Below 200 Hz the electric field spectral density is significantly larger outside the plasmasphere than inside the plasmasphere.

about 20 to 500 Hz with a maximum at about 62 Hz. This enhancement is produced by the low-frequency electric field noise bursts shown in Figure 2. The maximum integrated rms electric field strength for these low-frequency noise bursts is about 1 mv (meter)$^{-1}$.

Discussion

The most striking and unusual feature of these storm-time electric field observations is the occurrence of a region of intense low-frequency electric field noise bursts just outside the plasmapause boundary. These electric field noise bursts, which extend from about 20 to 500 Hz, are purely electrostatic and appear to be closely related to the occurrence of a magnetic storm, since no comparable noise bursts have been found during magnetically quiet periods. These noise bursts occur at the inner boundary of the proton ring current and in the region of steep proton intensity gradients reported by *Williams et al.* [1973]. The spatial correspondence between these two phenomena suggests that this electrostatic noise may be responsible for the pitch angle scattering and loss of ring current protons from the region near the plasmapause boundary during this storm. *Nagy et al.* [1972] have also reported a similar enhancement in the low-frequency (4 to 256 Hz) electric field intensities in association with an SAR-arc at low altitudes near the plasmapause boundary. These low-frequency noise bursts may possibly be related to the electrostatic plasma instability described by *Coroniti et al.* [1972]. The frequency range of this instability, which is between the ion cyclotron frequency and the ion plasma frequency, agrees reasonably well with the observed frequency range of the electric field noise bursts. The electric field amplitudes estimated by *Coroniti et al.* [1972] for this instability, 10 to 100 mv (meter)$^{-1}$, are, however, significantly larger than the broadband amplitudes, $\sim$1 mv (meter)$^{-1}$, which have been observed for this noise.

Acknowledgments. We wish to thank Drs. Laurence J. Cahill, Jr., and Nelson C. Maynard for letting us use their data in this paper.

This research was supported in part by the National Aeronautics and Space Administration under contract NAS5-11167 and grant NGL-16-001-043 and the Office of Naval Research under grant N00014-68-A-0196-0003.

References

Burtis, W. J., and R. A. Helliwell, Banded chorus—A new type of VLF radiation observed in the magnetosphere by OGO 1 and OGO 3, *J. Geophys. Res.*, *74*, 3002, 1969.

Carpenter, D. L., C. G. Park, H. A. Taylor, Jr., and H. C. Brinton, Multi-experiment detection of the plasmapause from EOGO satellites and Antarctic ground stations, *J. Geophys. Res.*, *74*, 1837, 1969.

Cornwall, J. M., F. V. Coroniti, and R. M. Thorne, Turbulent loss of ring current protons, *J. Geophys. Res.*, *75*, 4699, 1970.

Cornwall, J. M., F. V. Coroniti, and R. M. Thorne, Unified theory of SAR arc formation at the plasmapause, *J. Geophys. Res.*, *76*, 4428, 1971.

Coroniti, F. V., R. W. Fredricks, and Roscoe White, Electrostatic instability of ring current protons beyond the plasmapause during injection events, *TRW Systems Group Res. Rep. 22935-6001-R0-00*, May 1972.

Maynard, N. C., and D. P. Cauffman, Double floating probe measurements on S^3-A, *J. Geophys. Res.*, *78*, this issue, 1973.

Nagy, A. F., W. B. Hanson, T. L. Aggson, and R. J. Hoch, Satellite and ground-based observations of a red arc, *J. Geophys. Res.*, *77*, 3613, 1972.

Parady, B., and L. J. Cahill, Jr., ELF observations during the December 1971 storm, *J. Geophys. Res.*, *78*, this issue, 1973.

Russell, C. T., and R. E. Holzer, AC magnetic fields, in *Particles and Fields in the Magnetosphere*, edited by B. M. McCormac, p. 195, D. Reidel, Dordrecht, Holland, 1970.

Williams, D. J., T. A. Fritz, and A. Konradi, Observations of proton spectra ($1.0 \leq E_p \leq 300$ kev) and fluxes at the plasmapause, *J. Geophys. Res.*, *78*, this issue, 1973.

(Received July 26, 1972;
accepted February 28, 1973.)